ACADEMIC PRESS

Journal of Structural Biology 139 (2002) 46–54

Journal of Structural Biology

www.academicpress.com

Preliminary crystallographic analysis of the bacteriophage P22 portal protein

Gino Cingolani,[a] Sean D. Moore,[b,1] Peter E. Prevelige Jr.,[b] and John E. Johnson[a,*]

[a] *Department of Molecular Biology, The Scripps Research Institute, 10550 North Torrey Pines Road, La Jolla, CA 92037, USA*
[b] *Department of Microbiology, University of Alabama at Birmingham, Birmingham, AL 35294, USA*

Received 3 January 2002, and in revised form 25 April 2002

Abstract

Portal proteins are components of large oligomeric dsDNA pumps connecting the icosahedral capsid of tailed bacteriophages to the tail. Prior to the tail attachment, dsDNA is actively pumped through a central cavity formed by the subunits. We have studied the portal protein of bacteriophage P22, which is the largest connector characterized among the tailed bacteriophages. The molecular weight of the monomer is 82.7 kDa, and it spontaneously assembles into an oligomeric structure of approximately 1.0 MDa. Here we present a preliminary biochemical and crystallographic characterization of this large macromolecular complex. The main difficulties related to the crystallization of P22 portal protein lay in the intrinsic dynamic nature of the portal oligomer. Recombinant connectors assembled from portal monomers expressed in *Escherichia coli* form rings of different stoichiometry in solution, which cannot be separated on the basis of their size. To overcome this intrinsic heterogeneity we devised a biochemical purification that separates different ring populations on the basis of their charge. Small ordered crystals were grown from drops containing a high concentration of the kosmotropic agent *tert*-butanol and used for data collection. A preliminary crystallographic analysis to 7.0-Å resolution revealed that the P22 portal protein crystallized in space group *I*4 with unit cell dimensions $a = b = 409.4$ Å, $c = 260.4$ Å. This unit cell contains a total of eight connectors. Analysis of the noncrystallographic symmetry by the self-rotation function unambiguously confirmed that bacteriophage P22 portal protein is a dodecamer with a periodicity of 30°. The cryo-EM reconstruction of the dodecahedral bacteriophage T3 portal protein will be used as a model to initiate phase extension and structure determination.

Keywords: X-ray crystallography; Crystallization; Diffraction; P22 bacteriophage; Portal protein; Connector

1. Introduction

Portal proteins, also known as head-to-tail connectors, are large macromolecular oligomers found in all tailed bacteriophages. They are located at a single vertex of the icosahedral viral procapsid and present a characteristic architecture of a cone-shaped channel. Double-stranded DNA is pumped into the procapsid with a high level of efficiency (Smith et al., 2001) in a process that requires an accessory terminase complex and is powered by ATP hydrolysis (Casjens and Huang, 1982; Jackson et al., 1982). In addition to functioning as a DNA pump, portal proteins provide a docking site for the phage tail and also play a fundamental role in the assembly of the prohead (Bazinet and King, 1985).

Portal proteins from different bacteriophages differ significantly in size, charge distribution, and, at least in vitro, number of subunits forming the oligomer. The molecular mass of the portal monomer ranges from 35.9 kDa in φ29 to a maximum of 82.7 kDa in P22 (see Table 1). The oligomerization state of different portal proteins has been widely investigated, mostly by electron microscopy and image reconstruction for both wild-type and recombinant connectors. Twelvefold symmetric connectors were observed in bacteriophage T3 (Carazo et al., 1986), T4 (Driedonks, 1981), T7 (Kocsis et al., 1995), λ (Kochan et al., 1984), P22 (Bazinet et al., 1988), and φ29 (Guasch et al., 1998a,b; Valpuesta et al., 1999). However, mixed populations of 12 monomers and 13

* Corresponding author. Fax: +858-784-8660.
E-mail address: jackj@scripps.edu (J.E. Johnson).
[1] Present address: Department of Biology, MIT, Cambridge, MA 02139, USA.

1047-8477/02/$ - see front matter
PII: S1047-8477(02)00512-9

Table 1
Bacteriophage portal protein general composition

Bacteriophage	aa No.	MW subunit (kDa)[a]	Subunit No.	Isoelectric point[a]
ϕ29 (Guasch et al., 1998a,b)	309	35.9	12	5.03
P2 (Rishovd et al., 1998)	344	39.1	12/13	9.15
hk97 (Juhala et al., 2000)	424	47.2	?	7.94
SPP1 (Lurz et al., 2001; Dube et al., 1993)	503	57.3	12/13	4.26
T3 (Carazo et al., 1986)	535	58.6	12	4.38
T7 (Kocsis et al., 1995)	536	59.1	12/13	4.49
P22 (Bazinet et al., 1988)	725	82.7	12	4.55

[a] Molecular weight and predicted isoelectric point are calculated on the basis of the amino acid sequence using programs available at http://www.expacy.ch/.

monomers have been also reported for bacteriophages ϕ29 (Dube et al., 1993; Tsuprun et al., 1994), T7 (Cerritelli and Studier, 1996; Kocsis et al., 1995), and P2 (Rishovd et al., 1998). The unequivocal definition of the internal symmetry is made difficult by the size of the oligomer and, in the case of recombinant connector, by the purity and homogeneity of the rings. In the case of bacteriophage SPP1 portal protein, isolated recombinant portal rings (gp6) display 13-fold symmetry under all experimental conditions (Dube et al., 1993; Jekow et al., 1998; Orlova et al., 1999; Tsuprun et al., 1994). In contrast, gp6 has a 12-fold symmetric structure when imaged in the context of the viral connector, which also includes gp15 and gp16 (Lurz et al., 2001). This suggested that the viral assembly process may impose an oligomerization state on the portal protein different from that dictated by the protein assembly properties when isolated in solution. Based on a variety of studies of in vitro and in vivo assembled connector oligomers, the dodecamer appears to be the form present in the phage head, while other oligomeric states may form when the connector is assembled from recombinant protein.

Among all bacteriophage portal proteins, the best level of functional and structural understanding has been obtained for the bacteriophage ϕ29. The head-to-tail connector of this virus has been studied by atomic force microscopy (Valle et al., 1996), epitope mapping (Valle et al., 1999), cryoelectron microscopy and image processing (Carazo et al., 1986; Valpuesta et al., 1999) and X-ray crystallography (Badasso et al., 2000; Guasch et al., 1998a,b; Simpson et al., 2000, 2001). In the recently determined 2.9-Å crystal structure of ϕ29 bacteriophage portal protein (Simpson et al., 2000, 2001), the connector appears like a hollow funnel forming a 75-Å-long channel. In the oligomer, 12 subunits are intertwined to form three morphologically distinct domains: a wide crown-like domain of about 138 Å in diameter with protruding lobules, a middle domain, and a narrow cylindrical domain, approximately 66 Å in diameter. The secondary structure elements forming the three domains are also distinct, with both wide and narrow-end domains formed mostly by antiparallel β-sheets and the central domain made by a bundle of α-helices twisted in a left-handed fashion. Running through these three domains, there is a channel of about 40 Å in diameter that can easily accommodate double-stranded DNA. A cyclic RNA hexamer of 174 ribonucleotides, encoded by the ϕ29 genome and named prohead RNA (pRNA), is bound to the connector and is required for DNA packaging (Guo et al., 1987; Hendrix, 1998). Therefore the actual DNA-packaging machine used by ϕ29 is a ribonucleoprotein complex formed by the connector and the pRNA.

Different strategies are adopted by other tailed bacteriophages. In the case of P22, a bacteriophage that infects *Salmonella typhimurium*, portal protein is exclusively protein and accounts for an overall mass of approximately 1.0 MDa. Negatively stained micrographs of portal oligomers purified from virus revealed the existence of 12 arms and knobs projecting from a central ring. The approximate length of the channel is 130 Å while the central ring reaches about 180 Å in diameter (Bazinet et al., 1988). The assembly of bacteriophage P22 portal rings has been characterized biochemically in vitro using recombinant portal protein (Moore and Prevelige, 2001). Similar to connectors of other bacteriophages, the purified P22 portal monomer can assemble into a ring-like structure upon storage. The oligomerization process has been investigated by a variety of biophysical techniques including circular dichroism and Raman spectroscopies, thermal denaturation, and bis-ANS binding fluorescence. These studies suggested that the assembly of the monomeric subunit into the oligomeric structure is accompanied by significant structural changes (Moore and Prevelige, 2001; Rodriguez-Casado et al., 2001). While it appears that there may be a structurally conserved core between ϕ29 and P22 (Rodriguez-Casado et al., 2001), it remains unclear why in bacteriophage P22 the head-to-tail connector has such a large mass and whether there is any correlation between the size of the portal protein and the mechanism of phage maturation.

In this paper we present a preliminary biochemical and crystallographic analysis of the P22 portal protein. The P22 portal protein is the largest portal protein among the tailed bacteriophages and provides several interesting structural problems. We devised a strategy to

produce a homogenous population of recombinant P22 portal rings that we have crystallized in a highly concentrated solution of the kosmotropic agent *tert*-butanol. Small but ordered crystals of P22 bacteriophage portal protein were obtained and used for a preliminary X-ray analysis to 7 Å. Larger crystals have been subsequently obtained by fast reequilibration of the precipitant after formation of microcrystal nuclei. A preliminary analysis of the noncrystallographic symmetry by the self-rotation function confirmed that the P22 assembles head-to-tail into a dodecameric structure. We are currently using a pseudo-atomic model derived from a cryo-EM reconstruction of T3 portal protein (Valpuesta et al., 2000) to produce a molecular model suitable for structure determination.

2. Material and methods

2.1. Protein expression, purification, and ring assembly

Full-length P22 portal protein gene was previously cloned (Moore and Prevelige, 2001) in pET-21b vector (Novagen) and the recombinant histidine-tagged protein was expressed in *Escherichia coli* strain BL21 for 7 h at room temperature. Purification was performed on Qiagen Ni-agarose beads according to manufacturer's instructions. After extensive washing, the monomeric protein was eluted with elution buffer (70 mM sodium chloride, 20 mM Hepes, pH 7.5, 3 mM β-mercaptoethanol, 500 mM imidazole) and extensively dialyzed against Dialysis buffer (70 mM sodium chloride, 20 mM Hepes, pH 7.5, 3 mM β-mercaptoethanol, 1 mM EDTA). Portal monomers were then concentrated at $\sim$50 mg ml^{-1} using a Millipore concentrator (cut-off 50 kDa), and rings were formed by storage overnight at room temperature (Moore and Prevelige, 2001). After ring assembly, concentrated rings were centrifuged for 60 min at 25 000*g* to remove aggregate and further purified by gel filtration chromatography on a Superose 6 column (Pharmacia), previously equilibrated in crystallization buffer (70 mM sodium chloride, 20 mM Hepes, pH 7.5, 3 mM β-mercaptoethanol, 2.5 mM magnesium chloride). At this stage of the purification the portal protein appeared more than 99% pure on SDS–PAGE. A final round of ring purification by ion-exchange chromatography was carried out on a Mono Q column (Pharmacia), using a Pharmacia fast protein liquid chromatography system. Samples were applied to a Mono Q column preequilibrated in crystallization buffer and eluted with a continuous 70–1000 mM sodium chloride gradient at constant flow rate of 0.2 ml/min for 60 ml. Peak fractions (2) and (3) were pooled and concentrated using a Millipore concentrator (cut-off of 50 kDa), and the buffer was exchanged during concentration in crystallization buffer.

2.2. Crystallization

Crystallization trials were carried out by the sitting-drop vapor diffusion method at 20 and 4 °C. Screens 1 and 2 (Hampton Research) were employed to determine initial crystallization conditions. Prior to setting up crystallization drops, the removal of micro-aggregate by centrifugation was necessary to enable crystallization. The best crystals were obtained using 30–34% *tert*-butanol, 70 mM sodium chloride, 2.5% PEG 400 in 0.1 M sodium acetate, pH 5.6, with the portal ring at a concentration of $\sim$10 mg ml^{-1}. Usually 3 μl of P22 portal protein solution was mixed with 3 μl of reservoir solution and the mixture was maintained at 20 °C.

2.3. Synchrotron X-ray data collection and reduction

Data were collected from single small crystals mounted in a "cryoloop" (Hampton Research), quickly soaked in a cryoprotectant solution (30–34% *tert*-butanol, 70 mM sodium chloride, 25% PEG 400, and 100 mM sodium acetate, pH 5.6), and promptly frozen in a N_2 gas stream. X-ray data collection was carried out at BioCARS beamline 14BM-C, at the Advanced Photon Source, Argonne National Laboratories. Data were collected on an ADSC 232 CCD detector with monochromatic X rays at a wavelength of 1.0 Å and a detector to crystal distance of 425 mm. The oscillation angle used was $\sim$0.7° and the exposure time was 30 s per frame.

2.4. X-ray analysis

Data were processed and reduced with the *HKL* package (Otwinowski and Minor, 1997) and further analyzed with CCP4 programs (Collaborative Computational Project No. 4, 1994). The self-rotation function was computed with data between 10 and 7.5 Å resolution and a radius of integration of 60 Å using the program GLRF (Tong and Rossmann, 1997).

3. Results

3.1. Purification of homogenous oligomeric particles

Bacteriophage P22 portal monomer was overexpressed in *E. coli*, yielding over 100 mg of pure monomer per liter of *E. coli*. Portal subunits spontaneously assembled into rings when the concentration of the monomer was raised to 5–10 mg ml^{-1} (Moore and Prevelige, 2001). The purity and apparent homogeneity of the recombinant rings were confirmed by gel filtration chromatography, where the oligomeric connector migrated as a single species at the expected molecular size of $\sim$1 MDa (Fig. 1A). Despite the high solubility, purity,

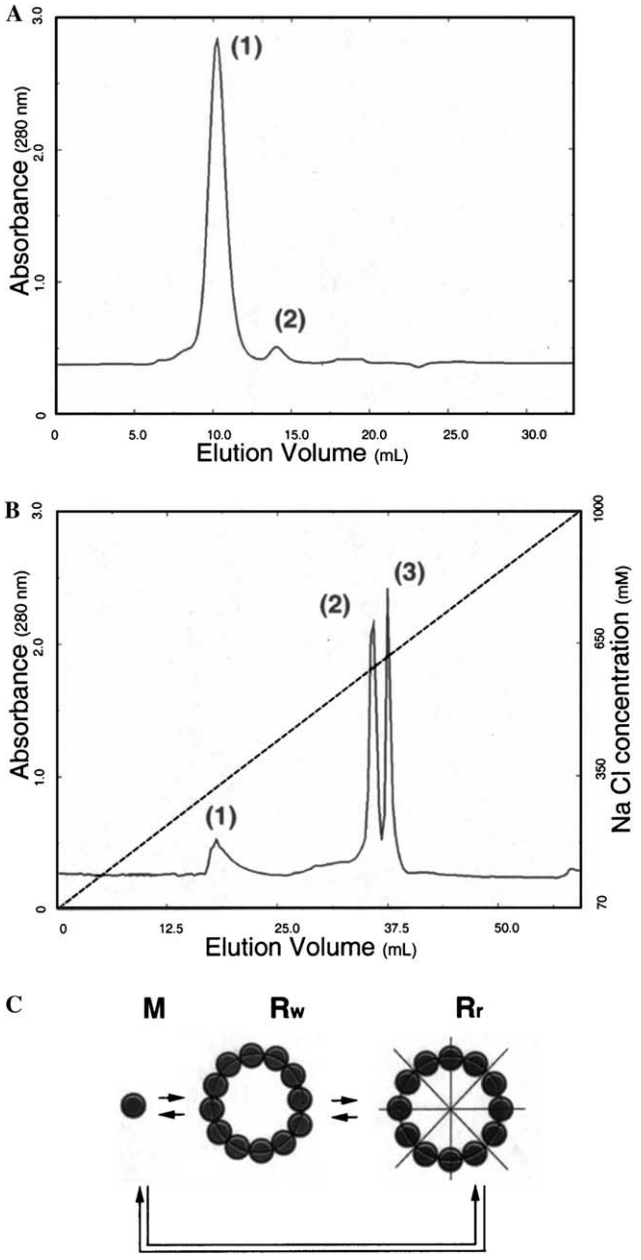

Fig. 1. Dynamic instability of bacteriophage P22 portal rings. (A) Gel filtration chromatogram of purified reassembled portal rings. (B) Separation of different subpopulations by ion-exchange chromatography. (C) Diagram showing the equilibrium existing among portal monomers (M), oligomeric particles formed by the correct number of subunits (R_r, right ring) and aberrant rings (R_w, wrong ring).

and salt stability of the P22 connector, extensive crystallization screenings were substantially unsuccessful. Only small nearly two-dimensional plate-like crystals were grown under highly concentrated alcohol solutions. However, these crystals were not reproducible, were difficult to manipulate and did not diffract X-rays. As the lack of homogeneity had been previously reported for recombinant portal proteins (Cerritelli and Studier, 1996; Kocsis et al., 1995; Rishovd et al., 1998), the poor quality of the crystals that we grew probably reflected the intrinsic heterogeneity of the rings formed by the recombinant oligomer. In order to select a homogeneous population of portal rings we took advantage of the acidic character of the portal monomer (the theoretical isoelectric point is ~4.7, see Table 1) and the salt resistance of the portal ring, which was stable in sodium chloride concentrations as high as ~600 mM. When a concentrated portal protein solution was injected onto an anion-exchange chromatography column and the bound protein was eluted with a sodium chloride gradient (about 60 bed volumes, see Section 2), three fractions were eluted, corresponding to peaks (1), (2), and (3) shown in Fig. 1B. The earliest peak, (1), eluted at ~400 mM sodium chloride, corresponding to the monomer. A second large peak was observed at a concentration of sodium chloride between 450 and 550 mM and finally a third peak was eluted at ~650 mM sodium chloride. The presence and position of peaks (2) and (3) varied substantially depending on the starting concentration of the portal ring loaded onto the column. At concentrations lower than 20 mg ml^{-1}, peak (2) appeared polydisperse in a range of salt concentrations ranging between 450 and 600 mM sodium chloride. In contrast, peak (3) appeared only when the rings were assembled from monomers concentrated to 40 mg ml^{-1}. If peaks (2) and (3) were analyzed on gel filtration chromatography under identical experimental conditions as in Fig. 1A, they migrated with an identical retention volume (data not shown), which was also indistinguishable from the heterogeneous ring prior to anion-exchange fractionation. The inability of gel filtration chromatography to resolve different populations of rings could be explained by the similar size of different oligomers. Even particles differing by one or more subunits were too similar to be resolved by gel filtration chromatography because of the poor separation power of gel filtration in this range of mass (~1 MDa). Alternatively it is possible that peaks (2) and (3) were in dynamic equilibrium in solution (Fig. 1C). In this case the single peak observed in Fig. 1A would reflect a mixture of different oligomers and not a single population of rings. The anion-exchange fractionation could separate distinct rings being adsorbed to the cationic matrix of the column and not in solution.

3.2. Crystallization of P22 connector under high concentration of the kosmotropic agent tert-butanol

To screen for crystallization, portal rings from both elution peaks (2) and (3) were desalted and concentrated to between 5 and 80 mg ml^{-1}. Peak (1) was not used as it contained only monomeric portal protein. For peaks (2) and (3) crystalloid precipitates appeared under several conditions at pH ~5.6 in the presence of *tert*-butanol (30–34%) and small amounts of polyethylene glycol 400

or ethylene glycol (2–2.5%). Crystals grew within 1–2 days and reached maximum size within a week. However, crystals from peak (2) grew with a plate-like morphology (typical size of $\sim 100 \times 40 \times 5\,\mu m^3$), similar to those obtained from portal protein not purified by anion-exchange chromatography, and diffracted X-rays only weakly. In contrast, crystallization droplets of connectors from peak (3) produced, under similar conditions, small bipyramidal crystals. These crystals showed clear edges and regular morphology, although only in the best cases did they reach 70 μm in the longest dimension (Fig. 2A), and they appeared within 8–12 weeks. Addition of additives such as magnesium chloride and calcium chloride did not appear to assist the crystallization.

Solutions highly concentrated in *tert*-butanol were previously reported for the crystallization of bacteriophage ϕ29 connector (Guasch et al., 1998a). This possible similarity suggests a correlation between the chemical properties of this compound and the crystallization of portal proteins. *Tert*-butanol is a kosmotrope and crowding agent (Franks and Reid, 1973), which acts, at room temperature, in water as a powerful "structure promoter." Like other kosmotropes, *tert*-butanol stabilizes proteins by decreasing their solubility and inducing salting-out. This effect is caused by the capacity of kosmotropes to exclude water from the surface of proteins, which are preferentially hydrated in an aqueous environment. Simultaneously, the exclusion of water promotes the folding by strengthening hydrophobic interactions at the protein–protein interface (Hope and Struhl, 1987; Jelesarov et al., 1998). In the case of large oligomeric assemblies like ϕ29 and P22 portal rings, crystallization under highly concentrated solutions of *tert*-butanol (up to 34%) could be explained by a synergistic effect of the *tert*-butanol in stabilizing the oligomerization of the portal monomer and salting-out the ring. The stabilization of the oligomer could be achieved by stabilizing hydrophobic interactions at the monomer:monomer interface, effectively reducing the intrinsic dynamic instability of the oligomer and "locking" the ring into a more discrete conformational state. Alternatively, the *tert*-butanol could induce crystallization by promoting the folding of a domain that is not present in the monomer but forms upon oligomerization. The latter is in good agreement with the observation that the oligomerization of P22 connector is accompanied by a significant gain in alpha-helical content (Moore and Prevelige, 2001), suggesting that the portal ring contains an ordered domain that is not present in the unassembled monomer. We are currently testing whether several other kosmotropic small ions (F^-, SO_4^{2-}, Li^+) of high density, well characterized for their properties of "water structure makers," could promote crystallization.

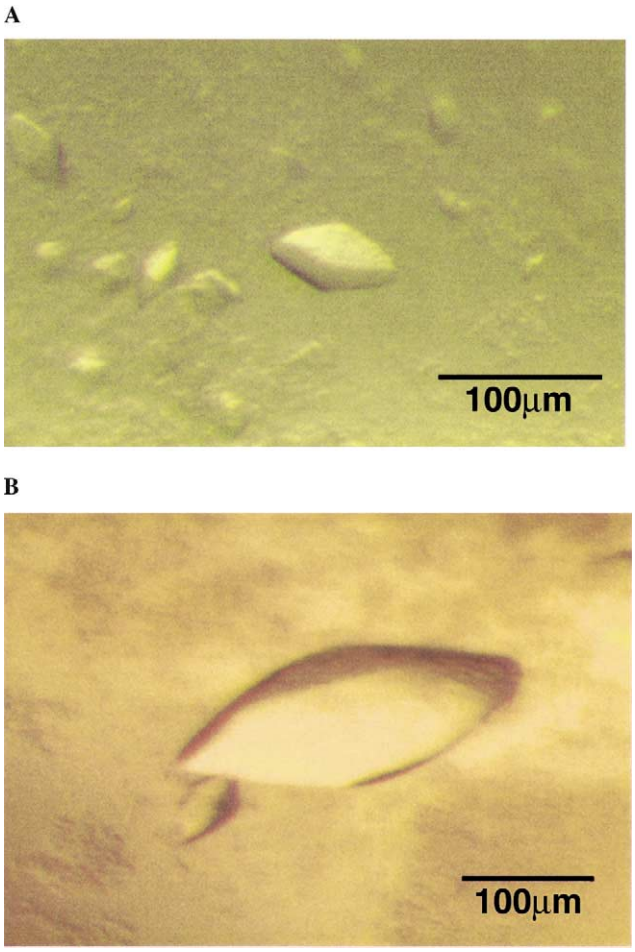

Fig. 2. Light micrographs of typical crystals of P22 bacteriophage portal ring. (A) Crystals were obtained by hanging-drop vapor diffusion and displayed bipyramidal morphology. The dimensions are approximately $70 \times 50 \times 40\,\mu m^3$. The hanging drops had a final volume of 3 μl and were set up by mixing equal amounts of protein and precipitant. (B) Portal protein crystals obtained after brief reequilibration of the droplet. The dimensions are approximately $300 \times 200 \times 120\,\mu m^3$ and displayed the same morphology of the microcrystal shown in Fig. 2A.

3.3. Growth of large crystals by reequilibration of the droplet

We found that crystallization was greatly enhanced by brief reequilibration of the crystallization droplet. Crystals as large as $\sim 300 \times 200 \times 120\ \mu m^3$ (Fig. 2B) were grown from the same droplets where the small bipyramidal crystals were found, simply by lifting the coverslip for few seconds. Since *tert*-butanol is a volatile compound, even a short reequilibration of the crystallization droplet could cause significant reduction of its concentration. As crystals appeared only at high concentrations of *tert*-butanol, it is plausible that high vapor pressure of the crystallization solution (30–34% *tert*-butanol) was needed to form crystal nuclei, while the actual growth of these nuclei was better achieved at a lower concentration of alcohol.

3.4. Data collection

Crystal harvesting was difficult because of the size of the crystals and the low viscosity of the crystallization precipitant. Moreover a thick film of precipitation often surrounded the crystals. We were able to harvest single crystals grown in the presence of 30–34% *tert*-butanol, quickly transfer them to stabilizing solutions containing crystallization buffer and 25% PEG 400, and freeze them under liquid nitrogen. Several data sets were collected at the Advanced Photon Source beamline 14-BM-C with a QUANTA CCD detector. As expected, the absolute intensity of the diffraction and resolution of the X-ray data appeared to be strongly correlated to the size of the crystal. The majority of the crystals with a maximum dimension of roughly 50 μm did not diffract beyond 12–15 Å resolution. A single crystal with overall dimensions of approximately $70 \times 40 \times 40\,\mu m^3$ diffracted X-rays to a maximum resolution of 7 Å. To accurately measure the low-resolution data the detector was placed 425 mm from the sample. Absorption of scattered X-rays by the air was minimized with a helium-filled aluminum cone placed between the crystal and detector. Over 500 images were recorded using an oscillation range of 0.7° and an exposure time of 30 s per image. A representative diffraction pattern is shown in Fig. 3. Despite the relative resolution of the crystal the diffraction patterns recorded displayed a distribution of diffraction maxima expected for a large macromolecular complex. Remarkably, despite the small size of the crystal (70 μm in the longest dimension) no significant radiation damage was observed during the data collection (total exposure time was about 4 h).

3.5. Data reduction

Over 500 frames were collected from a single frozen crystal and about 380 were used for data processing and scaling (Table 2). The crystal belonged to space group *I*4, with unit cell dimensions of $a = b = 409.4$ Å, $c = 260.4$ Å (Table 2). Over 6000 reflections were measured, corresponding to 33 551 unique reflections. Data are 100% complete in all shells from 60 to 7 Å and the redundancy of the data was roughly 18. As shown in Fig. 4B, the mean observed intensity was remarkably high, with the average I/σ_I for all reflections of 16.7 and about 2 in the highest resolution shell (7.3–7.0 Å resolution, Fig. 4B). Considering the unit cell edges of ~409 Å along crystallographic axes *a* and *b* and that the crystal used for data collection was only 70 μm along the longest dimension, the diffraction measured arose from an array of approximately 1700 unit cells, a remarkably small number when compared with the usual number of unit cells present in a typical protein crystal, which is estimated to be on the order of 10^9. Interestingly, analysis of scaling statistics revealed that the X-ray data were pseudo-*I*422, which differs from space group *I*4 by the presence of a twofold rotation axis along *x* and symmetry equivalent positions. In space group *I*422 the R_{merge} value is about 30% higher than in *I*4, probably demonstrating the approximate, but misaligned, twofold symmetry relating particles along the crystallographic axes. The average mosaic spread of the crystal, as defined by the program SCALEPACK (Otwinowski and Minor, 1997), was 0.35°. Assuming that a single portal ring consists of 12 subunits and has an overall molecular weight of about 1.0 MDa, and that a dimer of portal rings is present in the asymmetric unit of space group *I*4, the estimated volume per weight (V_m) is 2.8 Å Da^{-1} which is equivalent to a crystal solvent content of ~55%.

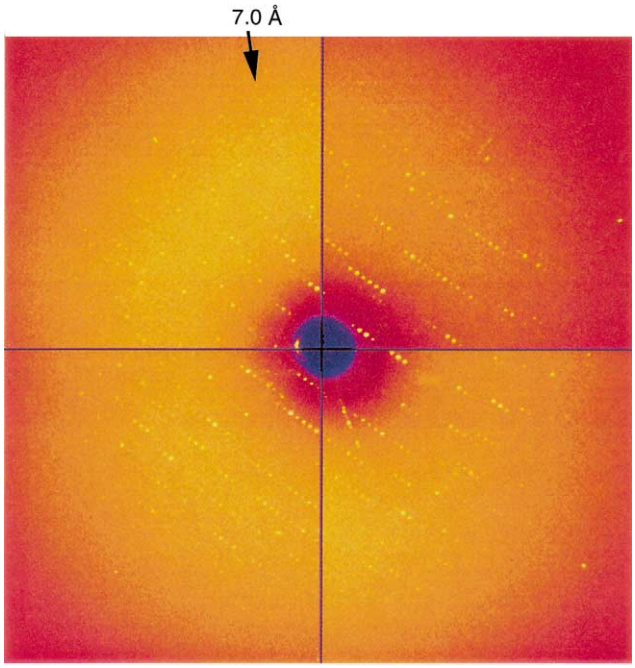

Fig. 3. A diffraction image recorded from bacteriophage P22 portal ring crystal oscillated 0.7° with an exposure time of 30 s. The X-ray wavelength was 1.0 Å and the crystal to detector distance was 425 mm. The vertical edge of the image corresponds to a resolution of 4.5 Å. Diffraction intensities can be accurately measured including a low resolution of ~60 Å.

Table 2
Summary of crystal data and diffraction statistics

Number of images	380
Space group	*I*4
Reflections (unique/total)	33 551/628 390
Redundancy	18
Unit cell	$a = 409.4$ Å; $b = 409.4$ Å; $c = 260.4$ Å
Resolution	60–7.0 Å (7.3–7.0 Å)
Completeness (%)	100 (100)
Rsym[a](%)	14.1 (80.1)
$\langle I/\sigma(I)\rangle$	16.7 (3.9)

Note. In parentheses are reported outer shell statistics.
[a] $R_{sym} = \sum i,h \mid I(i,h) - \langle I(h)\rangle \mid / \sum i,h \mid I(i,h) \mid$, where $I(i,h)$ and $\langle I(h)\rangle$ are the *i*th and mean measurements of intensity of reflection *h*.

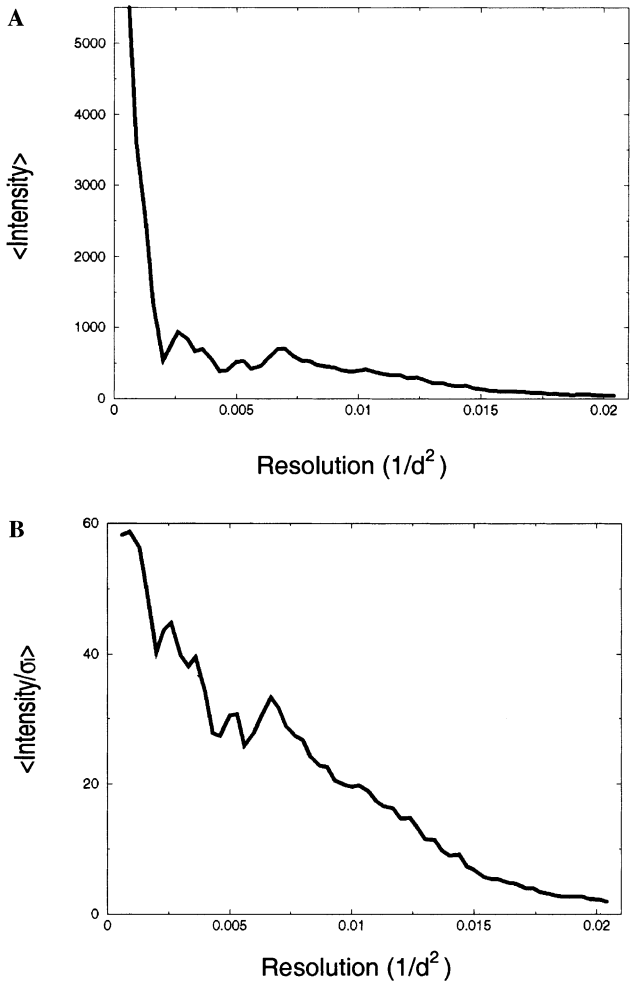

Fig. 4. The mean intensity plotted against resolution for observed X-ray data (A) in the resolution range 60–7 Å ($1/d^2 \sim 0.0006$–0.02). (B) The mean distribution of intensity normalized by the standard deviation of the error associated with the measured intensity is plotted versus the resolution ($1/d^2$). At 12-Å resolution the I/σ_I is larger than 12 and it drops to ~2 at 7 Å.

A complete summary of unit cell data and of the processing statistics is given in Table 2.

3.6. Analysis of non-crystallographic symmetry

The local symmetry in the connector was investigated by self-rotation functions (Rossmann and Blow, 1962) as implemented in the program GLRF (Tong and Rossmann, 1997) using polar angles. First we investigated the existence of local twofold axes of symmetry by computing a self-rotation function in space group $I4$ for $\kappa = 180°$. The best signal to noise was obtained including approximately 800 reflections with an I/σ_I higher than 5 in the resolution range 10–7.5 Å, which corresponds to about 10% of the reflections measured in this resolution range and using a radius of integration of 60 Å. As shown in Fig. 5A, the stereographic projections at $\kappa = 180°$ section revealed 2 orthogonal constellations

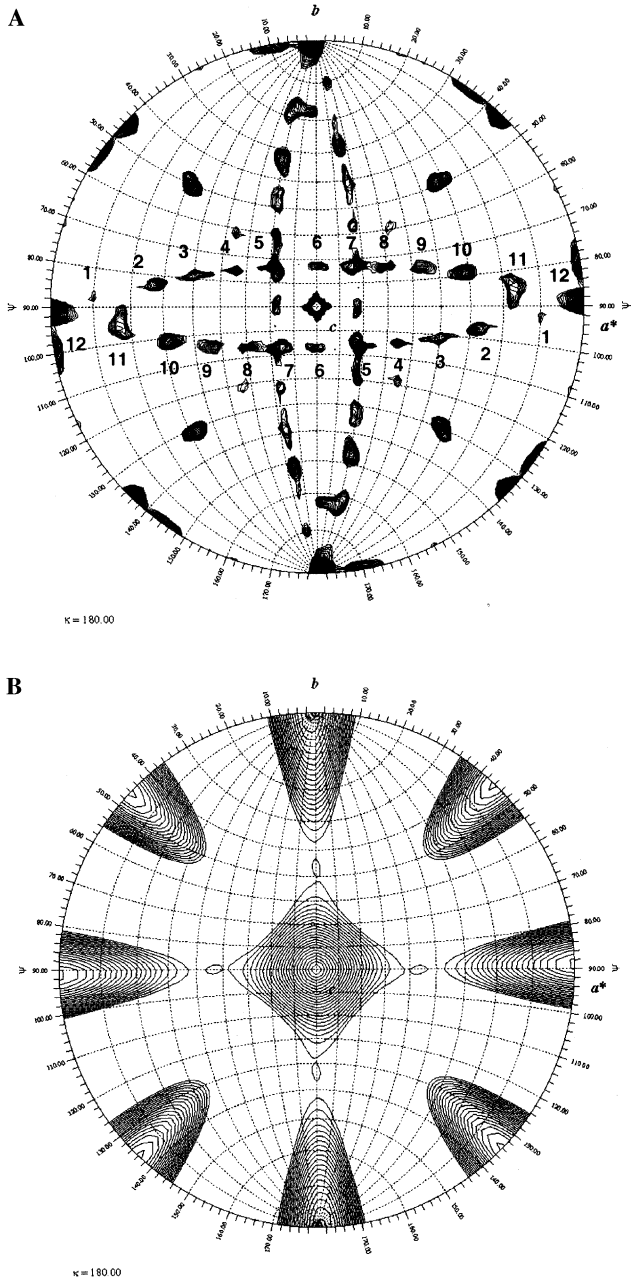

Fig. 5. Stereographic projections of the $k = 180°$ section of the P22 connector self-rotation function showing the direction of twofold axes of symmetry. The maps were contoured from 1σ to 15σ in steps of 0.25σ. The functions were computed with program GLRF (Tong and Rossmann, 1997) using a radius of integration of 60 Å. (A) Rotation function calculated with observed data between 10- and 7.5-Å resolution and calculated including low-resolution (B) data from 60- to 10-Å resolution. The eight large peaks represent the crystallographic eight symmetry operators present in space group $I4$.

of peaks, each representing an entire asymmetric unit. In each constellation 24 peaks were observed, representing the positions of two connectors in the asymmetric unit and suggesting that each connector was formed by 12 repeated subunits. Each peak was a maximum in the rotation function and resulted from the relationship

between the crystallographic fourfold axis (*c*-axis) and the 12-fold noncrystallographic symmetry axes running along the portal rings. This finding confirmed that the recombinant portal protein crystallized was an oligomeric assembly of 12 subunits, which agrees with the composition of wild-type connector purified from virus (Bazinet et al., 1988). Certain peaks were somewhat split, indicating that the two particles in the asymmetric unit were in similar but not identical twofold orientations. Interestingly, in a rotation function computed with only low-resolution data (10–60 Å), no 12-fold symmetry was visible (Fig. 5B). This was consistent with the fact that the low-resolution shell is dominated by solvent diffraction (Dodson, 2001). Here the 12-fold non crystallographic symmetry axis is obscured by the crystallographic symmetry. In this regard the eight peaks observed in Fig. 5B represent the eight symmetry operators of space group *I*4.

The stereographic plot allowed us to determine the orientation of the portal noncrystallographic 12-fold axis with respect to the crystallographic fourfold axis along the *c*-axis. The portal protein 12-fold axis is rotated approximately 17° from the crystallographic *b*-axis. Finally, to confirm the existence of a 12-fold symmetry axis, we computed a self-rotation function by fixing $\phi = -90°$ and $\psi = 17°$ and searched κ in the entire polar space 1°–360° (Fig. 6). This one-dimensional κ plot revealed, as expected, a regular periodicity of a maximum of the rotation function every 30°, confirming that the P22 bacteriophage portal protein is an oligomer of 12 subunits.

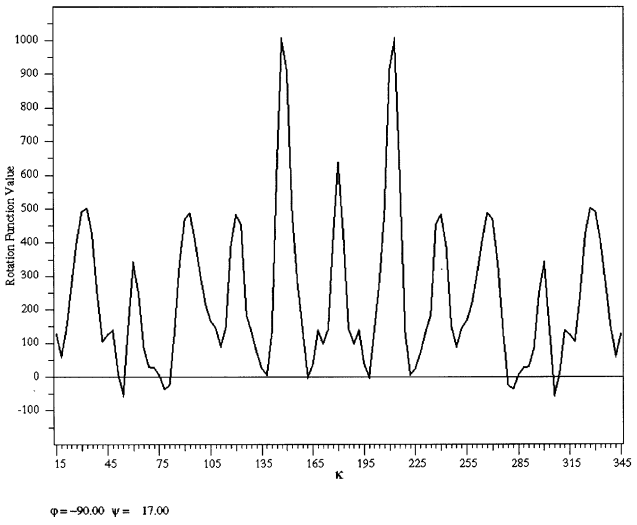

Fig. 6. One-dimensional plot showing the intensity of the rotation function at fixed values of $\phi = -90°$ and $\psi = 17°$ and searching κ from 0°–360°. The existence of a 12-fold noncrystallographic axis is suggested by the appearance of a maximum of the rotation function every 30°. The peak at the origin (0° = 360°) has been omitted for clarity. Here the rotation function has a maximum value.

4. Summary

Bacteriophage P22 portal protein is an interesting example of a viral molecular organization. A single viral gene encodes a polypeptide chain that contains all the information necessary to assemble into a highly symmetric macromolecular assembly. This structure plays a critical structural and functional role in virtually all stages of the virus replication cycle. Even though the thermodynamics of the connector self-assembly is partially understood (Moore and Prevelige, 2001; Rodriguez-Casado et al., 2001), the molecular mechanism of dsDNA pumping into a host cell is unknown. The crystal structure (Simpson et al., 2000) of ϕ29-bacteriophage connector provided valuable starting information about the overall architecture of dsDNA packaging motors. In the case of bacteriopage P22 portal protein, the major limitation in the study of the recombinant connector arises from the heterogeneity of the ring reassembled from *E. coli* expressed protein. Our inability to obtain crystals from connectors purified with a gel filtration column probably reflects the dynamic heterogeneity of the homo-oligomer and the constant interexchange of particles of similar size. It is reasonable to hypothesize that in vivo only oligomers formed by the "right" number of subunits will be assembled at the vertex to form a pro-head virion. The "quality-control" mechanism underlying this selection is likely to be dictated by the size of the capsid vertex itself, which can accommodate only particles with a defined number of subunits.

In this paper we have described a biochemical and preliminary crystallographic analysis of bacteriophage P22 head-to-tail connector. Our data have defined tractable targets for atomic-resolution structural analysis. In particular the biochemical basis for the homogenous formation of portal rings will be very useful for producing larger crystals that will yield a higher resolution than the actual 7 Å. Phase determination will be initiated with molecular-replacement real-space 24-fold averaging using the cryo-EM map of the T3 connector (Valpuesta et al., 2000).

Acknowledgments

We are grateful to the staff of BioCars on Sector 14 of the Advanced Photon Source for their help with data collection. The Advanced Photon Source is supported by the US Department of Energy, Basic Energy Sciences, Office of Science, under Contract W-31-109-Eng-38. Use of the BioCARS Sector 14 was supported by the National Institutes of Health, National Center for Research Resources, under Grant RR-07707. Gino Cingolani was supported by a "Human Frontier Science Program" post doctoral fellowship.

References

Badasso, M.O., Leiman, P.G., Tao, Y., He, Y., Ohlendorf, D.H., Rossmann, M.G., Anderson, D., 2000. Purification, crystallization and initial X-ray analysis of the head–tail connector of bacteriophage phi29. Acta Crystallogr. D Biol. Crystallogr. 56, 1187–1190.

Bazinet, C., King, J., 1985. The DNA translocating vertex of dsDNA bacteriophage. Annu. Rev. Microbiol. 39, 109–129.

Bazinet, C., Benbasat, J., King, J., Carazo, J.M., Carrascosa, J.L., 1988. Purification and organization of the gene 1 portal protein required for phage P22 DNA packaging. Biochemistry 27, 1849–1856.

Carazo, J.M., Fujisawa, H., Nakasu, S., Carrascosa, J.L., 1986. Bacteriophage T3 gene 8 product oligomer structure. J. Ultrastruct. Mol. Struct. Res. 94, 105–113.

Casjens, S., Huang, W.M., 1982. Initiation of sequential packaging of bacteriophage P22 DNA. J. Mol. Biol. 157, 287–298.

Cerritelli, M.E., Studier, F.W., 1996. Purification and characterization of T7 head–tail connectors expressed from the cloned gene. J. Mol. Biol. 258, 299–307.

Collaborative Computational Project No. 4 (1994). The CCP4 suite: programs for protein crystallography. Acta Crystallogr. D 50, 760–763.

Dodson, E.J., 2001. Using electron-microscopy images as a model for molecular replacement. Acta Crystallogr. D Biol. Crystallogr. 57, 1405–1409.

Driedonks, R.A., 1981. The quaternary structure of the T4 gene product 20 oligomer. Prog. Clin. Biol. Res. 64, 315–323.

Dube, P., Tavares, P., Lurz, R., vanHeel, M., 1993. The portal protein of bacteriophage SPP1: a DNA pump with 13-fold symmetry. EMBO J. 12, 1303–1309.

Franks, F., Reid, D.S., 1973. In: Franks, F. (Ed.), Thermodynamic Properties in Water. A comprehensive Treatise: Water in Crystalline Hydrate: Aqueous Solution of Simple Nonelectrolytes. Plenum, New York, pp. 323–380.

Guasch, A., Parraga, A., Pous, J., Valpuesta, J.M., Carrascosa, J.L., Coll, M., 1998a. Purification, crystallization and preliminary X-ray diffraction studies of the bacteriophage phi29 connector particle. FEBS Lett. 430, 283–287.

Guasch, A., Pous, J., Parraga, A., Valpuesta, J.M., Carrascosa, J.L., Coll, M., 1998b. Crystallographic analysis reveals the 12-fold symmetry of the bacteriophage phi 29 connector particle. J. Mol. Biol. 281, 219–225.

Guo, P.X., Erickson, S., Anderson, D., 1987. A small viral RNA is required for in vitro packaging of bacteriophage phi29 DNA. Science 236, 690–694.

Hendrix, R.W., 1998. Bacteriophage DNA packaging: RNA gears in a DNA transport machine. Cell 94, 147–150.

Hope, I.A., Struhl, K., 1987. GCN4, a eukaryotic transcriptional activator protein, binds as a dimer to target DNA. EMBO J. 6, 2781–2784.

Jackson, E.N., Laski, F., Andres, C., 1982. Bacteriophage P22 mutants that alter the specificity of DNA packaging. J. Mol. Biol. 154, 551–563.

Jelesarov, I., Durr, E., Thomas, R.M., Bosshard, H.R., 1998. Salt effects on hydrophobic interaction and charge screening in the folding of a negatively charged peptide to a coiled coil (leucine zipper). Biochemistry 37, 7539–7550.

Jekow, P., Schaper, S., Gunther, D., Tavares, P., Hinrichs, W., 1998. Crystallization and preliminary X-ray crystallographic studies of the 13-fold symmetric portal protein of bacteriophage SPP1. Acta Crystallogr. D Biol. Crystallogr. 54, 1008–1011.

Juhala, R., Ford, M.E., Duda, R.L., Youlton, A., Hatfull, G.F., Hendrix, R.W., 2000. Genomic sequences of bacteriophages HK97 and HK022: pervasive genetic mosaicism in the lambdoid bacteriophages. J. Mol. Biol. 299, 27–51.

Kochan, J., Carrascosa, J.L., Murialdo, H., 1984. Bacteriophage lambda preconnectors. Purification and structure. J. Mol. Biol. 174, 433–447.

Kocsis, E., Cerritelli, M.E., Trus, B.L., Cheng, N., Steven, A.C., 1995. Improved methods for determination of rotational symmetries in macromolecules. Ultramicroscopy 60, 219–228.

Lurz, R., Orlova, E.V., Gunther, D., Dube, P., Droge, A., Weise, F., van Heel, M., Tavares, P., 2001. Structural organisation of the head-to-tail interface of a bacterial virus. J. Mol. Biol. 310, 1027–1037.

Moore, S.D., Prevelige Jr., P.E., 2001. Structural transformations accompanying the assembly of bacteriophage P22 portal protein rings in vitro. J. Biol. Chem. 276, 6779–6788.

Orlova, E.V., Dube, P., Beckmann, E., Zemlin, F., Lurz, R., Trautner, T.A., Tavares, P., van Heel, M., 1999. Structure of the 13-fold symmetric portal protein of bacteriophage SPP1. Nat. Struct. Biol. 6, 842–846.

Otwinowski, Z., Minor, W., 1997. Processing of X-ray diffraction data collected in oscillation mode. Methods Enzymol. 276, 307–326.

Rishovd, S., Holzenburg, A., Johansen, B.V., Lindqvist, B.H., 1998. Bacteriophage P2 and P4 morphogenesis: structure and function of the connector. Virology 25, 11–17.

Rodriguez-Casado, A., Moore, S.D., Prevelige Jr., P.E., Thomas, G.J., 2001. Structure of bacteriophage p22 portal protein in relation to assembly: investigation by Raman spectroscopy. Biochemistry 40, 13583–13591.

Rossmann, M., Blow, D.M., 1962. The detection of sub-units within the crystallographic asymmetric unit. Acta Crystallogr. 15, 24–31.

Simpson, A.A., Leiman, P.G., Tao, Y., He, Y., Badasso, M.O., Jardine, P.J., Anderson, D.L., Rossmann, M.G., 2001. Structure determination of the head–tail connector of bacteriophage varphi29. Acta Crystallogr. D Biol. Crystallogr. 57, 1260–1269.

Simpson, A.A., Tao, Y., Leiman, P.G., Badasso, M.O., He, Y., Jardine, P.J., Olson, N.H., Morais, M.C., Grimes, S., Anderson, D.L., Baker, T.S., Rossmann, M.G., 2000. Structure of the bacteriophage phi29 DNA packaging motor. Nature 408, 745–750.

Smith, D.E., Tans, S.J., Smith, S.B., Grimes, S., Anderson, D.L., Bustamante, C., 2001. The bacteriophage straight phi29 portal motor can package DNA against a large internal force. Nature 413, 748–752.

Tong, L., Rossmann, M.G., 1997. Rotation function calculations with GLRF program. Methods Enzymol. 276, 594–611.

Tsuprun, V., Anderson, D., Egelman, E.H., 1994. The bacteriophage phi 29 head–tail connector shows 13-fold symmetry in both hexagonally packed arrays and as single particles. Biophys. J. 66, 2139–2150.

Valle, M., Kremer, L., Martinez, A.C., Roncal, F., Valpuesta, J.M., Albar, J.P., Carrascosa, J.L., 1999. Domain architecture of the bacteriophage phi29 connector protein. J. Mol. Biol. 288, 899–909.

Valle, M., Valpuesta, J.M., Carrascosa, J.L., Tamayo, J., Garcia, R., 1996. The interaction of DNA with bacteriophage phi 29 connector: a study by AFM and TEM. J. Struct. Biol. 116, 390–398.

Valpuesta, J.M., Fernandez, J.J., Carazo, J.M., Carrascosa, J.L., 1999. The three-dimensional structure of a DNA translocating machine at 10 Å resolution. Struct. Fold. Des. 7, 289–296.

Valpuesta, J.M., Sousa, N., Barthelemy, I., Fernandez, J.J., Fujisawa, H., Ibarra, B., Carrascosa, J.L., 2000. Structural analysis of the bacteriophage T3 head-to-tail connector. J. Struct. Biol. 131, 146–155.